

# CHEMISTRY

## A European Journal

A Journal of



### Accepted Article

**Title:** [2.2]Paracyclophanes with N-Heterocycles as Ligands for Mono- and Dinuclear Ruthenium(II) Complexes

**Authors:** Carolin Braun, Martin Nieger, Werner R. Thiel, and Stefan Bräse

This manuscript has been accepted after peer review and appears as an Accepted Article online prior to editing, proofing, and formal publication of the final Version of Record (VoR). This work is currently citable by using the Digital Object Identifier (DOI) given below. The VoR will be published online in Early View as soon as possible and may be different to this Accepted Article as a result of editing. Readers should obtain the VoR from the journal website shown below when it is published to ensure accuracy of information. The authors are responsible for the content of this Accepted Article.

**To be cited as:** *Chem. Eur. J.* 10.1002/chem.201703291

**Link to VoR:** <http://dx.doi.org/10.1002/chem.201703291>

Supported by  
**ACES**

WILEY-VCH

## FULL PAPER

[2.2]Paracyclophanes with *N*-Heterocycles as Ligands for Mono- and Dinuclear Ruthenium(II) ComplexesCarolin Braun,<sup>[a]</sup> Martin Nieger,<sup>[b]</sup> Werner R. Thiel<sup>[c]</sup> and Stefan Bräse\*<sup>[a,d]</sup>

**Abstract:** [2.2]Paracyclophane, with its unique structure, allows the design of unusual 3D structures by functionalization of this rigid and stable hydrocarbon scaffold. Therefore different mono- and homodisubstituted [2.2]paracyclophanes with pyridyl, pyrimidyl and oxazolonyl substituents were developed in order to evaluate their ability as bridging ligands for two ruthenium centres. With the successfully synthesized [2.2]paracyclophane-based *N*-donor functions, the cycloruthenation reaction using  $[\text{RuCl}_2(\rho\text{-cymene})]_2$  as precursor was explored. Compared to 2-phenylpyridine, the [2.2]paracyclophane derivative is clearly inferior in the cycloruthenation reaction, resulting in poor yields for the neutral complexes. By addition of  $\text{KPF}_6$ , the cationic complexes can be obtained in good yields and are formed diastereoselectively in case of a pyridyl substituent, resulting in only one diastereomer for dinuclear ruthenium complexes of bispyridyl-substituted [2.2]paracyclophanes as bridging ligands.

## Introduction

Since the discovery of the [2.2]paracyclophane scaffold by Brown and Farthing in 1949<sup>[1]</sup> and the pioneering work of Reich and Cram,<sup>[2]</sup> this class of bridged aromatic compounds has been extensively studied in terms of reactivity<sup>[3]</sup>, properties<sup>[4]</sup>, its use for planar-chiral ligands<sup>[5]</sup> as well as for material science<sup>[6]</sup>. Because of its unique 3D structure, [2.2]paracyclophanes feature trans-annular properties which impart exceptional reactivity and make it attractive as building block for complex molecules with an unusual and rigid spatial structure. The [2.2]paracyclophane backbone enables the design of bridging ligands in which the position of two transition metals is controlled. Because of the well-known stability

of five-membered metallacycles, [2.2]paracyclophanes attached to *N*-heterocycles that possess a  $\text{sp}^2$ -nitrogen in *ortho*-position are of particular interest. Therefore we chose pyridine, pyrimidine and oxazoline rings as preferred substituents (**Figure 1**), which have the advantage that synthetic routes to their monosubstituted [2.2]paracyclophane derivatives are well established. Furthermore, the ability of the oxazoline<sup>[7]</sup> and the pyridine<sup>[8]</sup> derivative to coordinate transition metals like palladium to yield complexes like **1**<sup>[7]</sup> and **2**<sup>[9]</sup> have been already reported. Therefore the formation of dinuclear metal complexes with an appropriate ligand system is very likely. As a result of the particular structure of [2.2]paracyclophane, a greater variety of disubstituted regioisomers are accessible than in the analogous phenyl molecules. Some of these isomers possess planar chirality depending on the substituents and their connectivity. Among homodisubstituted [2.2]paracyclophanes, achiral pseudo-*para* derivatives are most desirable as they are readily accessible from the respective dibromide.<sup>[3]</sup> In case of their double cyclometallation, the metal centres are not able to interact directly. With a *para*-disubstituted derivative, the two metal centres are situated at the same phenyl ring changing their electronic environment.

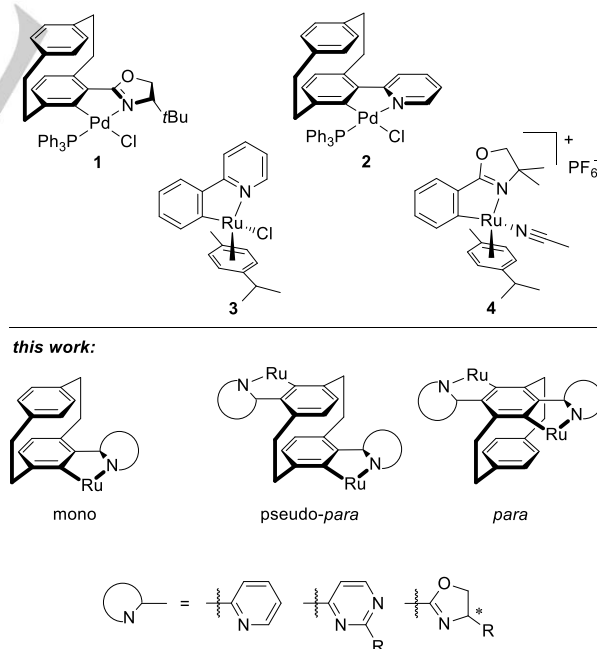


**Figure 1:** Known cyclopalladated [2.2]paracyclophanes **1**<sup>[7]</sup> and **2**<sup>[9]</sup>, cycloruthenated phenylpyridine **3**<sup>[10]</sup> and phenyloxazoline **4**<sup>[11]</sup> as starting point for the development of [2.2]paracyclophane-based mono- and dinuclear ruthenium complexes.

- [a] C. Braun, Prof. Dr. S. Bräse  
Institute of Organic Chemistry  
Karlsruhe Institute of Technology (KIT)  
Fritz-Haber-Weg 6, 76131 Karlsruhe, Germany  
E-mail: braese@kit.edu
- [b] Dr. M. Nieger  
Department of Chemistry, University of Helsinki  
P.O. Box 55, 00014 University of Helsinki, Finland
- [c] Prof. Dr. Werner R. Thiel  
Fachbereich Chemie, Technische Universität Kaiserslautern  
Erwin-Schrödinger-Straße 54, 67663 Kaiserslautern, Germany
- [d] Prof. Dr. S. Bräse  
Institute of Toxicology and Genetics  
Karlsruhe Institute of Technology (KIT)  
Hermann-von-Helmholtz-Platz 1, 76344 Eggenstein-Leopoldshafen, Germany

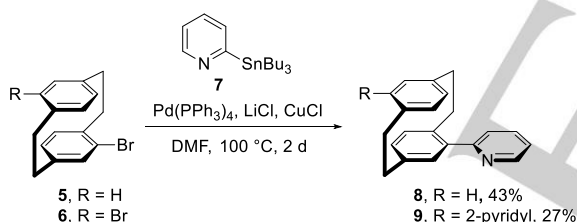
Supporting information for this article is given via a link at the end of the document.

## FULL PAPER

To explore the suitability of biscyclometallated [2.2]paracyclophanes as bridging ligands with unique electronic properties, we selected ruthenium(II) as diamagnetic transition metal centre. On the one hand ruthenium(II) is known to form defined monomeric complexes like **3**<sup>[10]</sup> and **4**<sup>[11]</sup> with the phenyl derivatives, on the other hand, ruthenium(II)-complexes with an  $\eta^6$ -coordinated *p*-cymene ligand are usually air- and moisture stable. Therefore we developed synthetic routes to pseudo-*para*- and *para*-disubstituted [2.2]paracyclophanes that are potentially bridging ligands for dinuclear transition metal complexes and explored their coordination behavior for the cyclometallation of ruthenium(II).

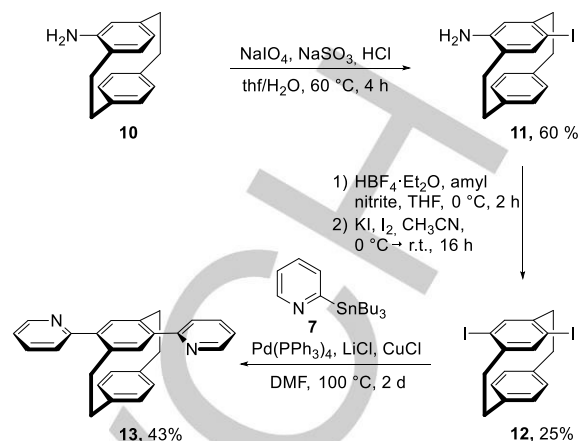
## Results and Discussion

**Synthesis of pyridyl-substituted [2.2]paracyclophanes.** In order to develop [2.2]paracyclophanes as bridging ligands, we synthesized the different mono- and homodisubstituted [2.2]paracyclophanes. As previously shown, pyridyl substituents are easily accessible *via* Stille cross coupling reactions in only one step (Scheme 1).<sup>[8b]</sup> This makes these substituents attractive as they can be easily varied with respect to subsequent fine-tuning of this ligand type. We already reported the synthesis for mono- and pseudo-*para*-bispyridyl-substituted [2.2]paracyclophanes **8** and **9** from the respective bromides **5** and **6**. They are accessible from commercially available unsubstituted [2.2]paracyclophane *via* single or double bromination adjusting the reaction conditions and workup procedures.<sup>[2c-e, 12]</sup>



**Scheme 1:** Synthesis of 2-pyridyl-substituted [2.2]paracyclophanes **8** and **9** *via* Stille cross coupling.<sup>[8b]</sup>

However, during the double bromination of unsubstituted [2.2]paracyclophane the *para*-dibromide is only a side product and its separation from the other side products of the unselective bromination is not trivial. As a result, we required a different approach to such *para*-homodisubstituted [2.2]paracyclophanes and developed a synthetic route towards the *para*-diiodo-[2.2]paracyclophane (**12**, Scheme 2). This *para*-diiodide **12** was obtained by *para*-iodination of the aniline derivative **10** followed by the Sandmeyer-type reaction of amine **11**. The *para*-bispyridyl-substituted [2.2]paracyclophane **13** could be prepared from the diiodo species **12** in one step by a Stille cross coupling reaction. We could obtain the molecular structure of the diiodide **12** as well as the cross coupling product **13** by X-ray crystallography both confirming the *para*-disubstitution (the crystal structure of **12** can be found in the supporting information).



**Scheme 2:** Synthesis of *para*-diiodide **12** as substrate for the Stille cross coupling reaction to yield **13**.

In case of the bispyridyl-substituted **13** (Figure 2), the molecule shows the characteristic twist between the pyridyl rings and the [2.2]paracyclophane backbone, which was reported for the mono- and pseudo-*para*-disubstituted [2.2]paracyclophanes.<sup>[8b]</sup> Noteworthy, with 32.3° and 44.1° two different angles were observed for the twist of the two pyridyl substituents towards the [2.2]paracyclophane backbone, whereas for the pseudo-*para*-derivative **6a** they show the same angle of 37.2°.<sup>[8b]</sup>

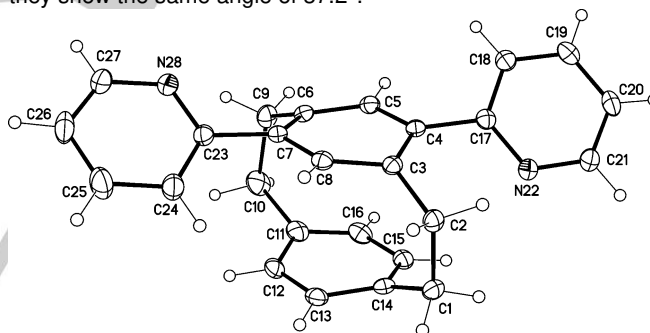
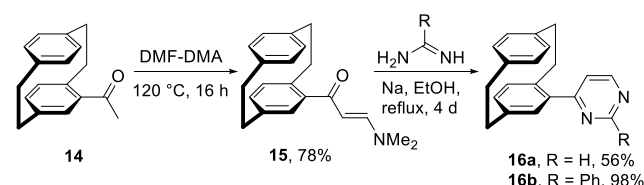


**Figure 2:** Molecular structure of bispyridyl[2.2]paracyclophane **13** (displacement parameters are drawn at 50% probability level).

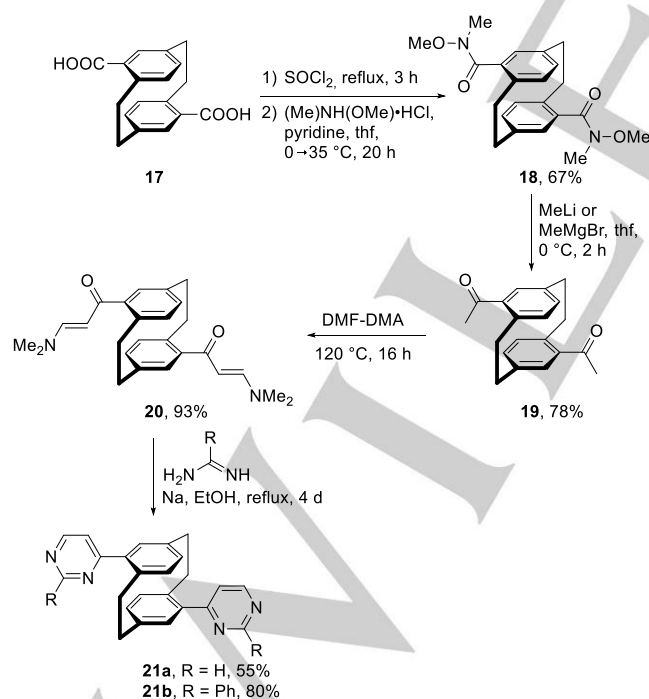
**Synthesis of pyrimidyl-substituted [2.2]paracyclophanes.** After we had successfully synthesized the desired pyridyl-substituted derivatives, we focused on the preparation of the pyrimidyl-substituted [2.2]paracyclophanes.



**Scheme 3:** Synthesis of pyrimidyl-substituted [2.2]paracyclophanes **16** *via* enaminone **15**.

## FULL PAPER

The *de novo* synthesis of pyrimidine rings starting from enaminones and amidines is well established,<sup>[13]</sup> and our group already reported the synthesis of monopyrimidyl-substituted [2.2]paracyclophanes **16** from the 4-acetyl[2.2]paracyclophane (**14**, **Scheme 3**).<sup>[14]</sup> A X-ray crystal structure could be obtained from **16a** that confirms the molecular structure and shows a twist of the pyrimidyl ring against the [2.2]paracyclophane backbone of 37.8° (see supporting information for more details). The disubstituted derivatives should be accessible by the same synthetic route from the respective diacetyl[2.2]paracyclophane. Unfortunately, the synthesis of diacetyl-substituted [2.2]paracyclophanes is challenging because the Friedel-Crafts acylation gives the monoacetylated product **14** selectively due to transannular effects between the two phenyl rings of the [2.2]paracyclophane backbone.<sup>[15]</sup> Another possibility to prepare the monoacetylated [2.2]paracyclophane is the reaction of the carboxy[2.2]paracyclophane with methyl lithium.<sup>[16]</sup> In case of the pseudo-*para*-dicarboxylic acid **17**, the pseudo-*para*-diacetyl[2.2]paracyclophane **19** was obtained only with a maximum yield of 6% by reaction with methyl lithium, probably due to the very low solubility of **17** in thf or diethyl ether. Therefore we adjusted our reaction sequence and could successfully synthesize the diacetylated [2.2]paracyclophane **19** via the Weinreb amide **18**, which could be converted to **19** in good overall yield by reaction with methyl magnesium bromide or methyl lithium (**Scheme 4**). Afterwards, the synthesis of the bispyrimidyl-substituted [2.2]paracyclophanes **21** could be completed by reaction with dimethylformamide dimethyl acetal (DMF-DMA) to the enaminone **20**, that is subsequently converted to the bispyrimidyl-substituted [2.2]paracyclophanes by reaction with formamidine (**21a**) or benzamidine (**21b**) in moderate to good yield.



**Scheme 4:** Synthesis of pseudo-*para*-bispyrimidyl-substituted [2.2]paracyclophanes **21** with the diacetylated [2.2]paracyclophane **18** as key intermediate.

For **18**, **19** and **21b** the molecular structures by X-ray crystallography confirm the pseudo-*para*-disubstitution of the [2.2]paracyclophane backbone (see supporting information for details about the molecular structures of **18** and **19**). The molecular structure of **21b** for one of the two independent molecules per unit cell is shown in **Figure 3**. The observed conformations of the bispyridyl-<sup>[8b]</sup> and bispyrimidyl-substituted [2.2]paracyclophanes can be explained by minimization of the dipoles and packing effects in the solid state.

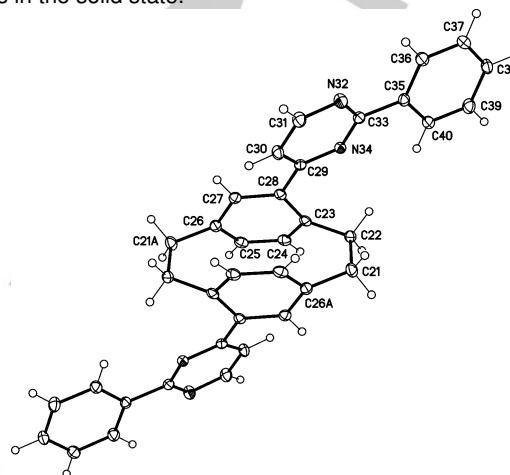
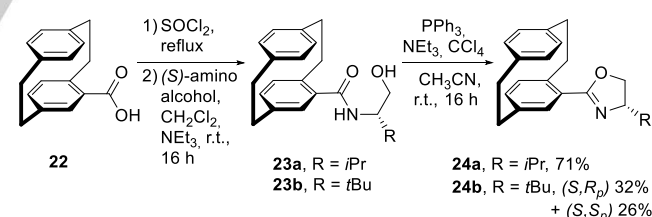
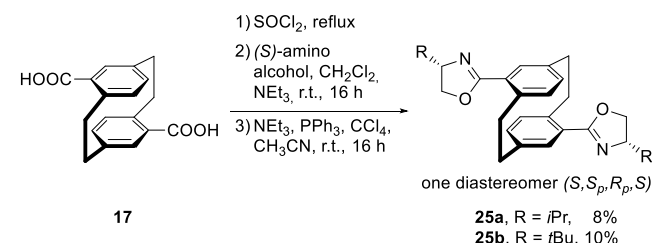


**Figure 3:** Molecular structure of **21b** (displacement parameters are drawn at 50% probability level). For clarity only one of the two independent molecules per unit cell is shown.

**Oxazoliny-substituted [2.2]paracyclophanes.** Moreover we introduced oxazoliny substituents into the [2.2]paracyclophane scaffold. Monooxazoliny-substituted [2.2]paracyclophanes **24** are well-known and could be readily prepared from the carboxy[2.2]paracyclophane **22** (**Scheme 5**).<sup>[7, 17]</sup>



**Scheme 5:** Synthesis of oxazoliny-substituted [2.2]paracyclophanes **24**.

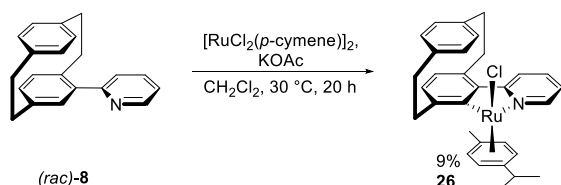


**Scheme 6:** Synthesis of bisoxazoliny-substituted [2.2]paracyclophanes **25** starting from dicarboxylic acid **17**.

## FULL PAPER

The analogous reaction sequence was applied for the synthesis of the pseudo-*para*-bisoxazolines, starting from the pseudo-*para*-dicarboxylic acid **17** (Scheme 6). This reaction illustrates clearly the peculiarity of planar-chiral substituted [2.2]paracyclophanes. Through twofold reaction of the achiral acid **17**<sup>[18]</sup> with the (*S*)-amino alcohol, the original *C<sub>i</sub>* symmetry is broken, resulting one chiral (*S<sub>p</sub>,R<sub>p</sub>,S*)-diastereomer of **25a** and **b**.

**Cycloruthenation of the [2.2]paracyclophane scaffold.** After completing our ligand synthesis we focused our efforts on the synthesis of the intended ruthenium(II) complexes. Numerous procedures exist in the literature for the synthesis of neutral ruthenium(II) complexes of 2-phenylpyridines, such as **3**, in high yields (>90%), each using 0.5 equiv. of the dimeric ruthenium precursor and a variable amount of a base.<sup>[10b, 19]</sup> Therefore we tried analogous reaction conditions for the cycloruthenation of our racemic 2-pyridyl-substituted [2.2]paracyclophane (*rac*)-**8**, but our efforts did not result in yields higher than 9% (Scheme 7, see supporting information for more details).



Scheme 7: Cycloruthenation of **8** with  $[\text{RuCl}_2(p\text{-cymene})]_2$ .

Coordination of **8** to the ruthenium(II) centre creates a new stereogenic centre as the metal has a pseudo-tetrahedral “piano stool” coordination geometry. In conjunction with the stereogenic plane of [2.2]paracyclophane this could potentially lead to diastereomers. The NMR spectra do not show any evidence for a diastereomeric product mixture, indicating that a diastereoselective cycloruthenation took place. A plausible reason for a single diastereomer involves the interaction of the [2.2]paracyclophane framework and the *p*-cymene ligand. With both coordinated to the ruthenium centre, and the [2.2]paracyclophane in a bidentate fashion, there is no freedom in the (*R<sub>p</sub><sup>\*</sup>,S<sup>\*</sup>*)-diastereomer for the *p*-cymene ligand to avoid non-bonding interactions with the core of the paracyclophane (Figure 4). In contrast, in the (*R<sub>p</sub><sup>\*</sup>,R<sup>\*</sup>*)-diastereomer the *p*-cymene is orientated away from both decks of the paracyclophane and is therefore the more stable product. For this discussion only the relative configuration is stated, and all contemplations pertain inversely to the other enantiomer.

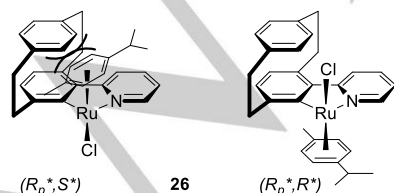
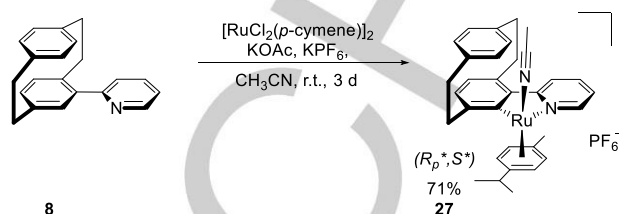


Figure 4: The two diastereomers of the ruthenium complex **26** and a possible explanation for the preference for (*R<sub>p</sub><sup>\*</sup>,S<sup>\*</sup>*). The relative configuration is shown.

The yield of **26** is far from satisfactory, so we investigated alternative methods to form ruthenium(II) complexes. The literature contains a multitude of possible solutions<sup>[20]</sup> with the most favourable appearing to be the preparation of cationic complexes as reported by Pfeffer and Le Lagadec.<sup>[21]</sup>



Scheme 8: Synthesis of the cationic ruthenium(II) complex **27**. The relative configuration is shown.

By addition of potassium hexafluorophosphate to the reaction mixture, we were able to approach cycloruthenated [2.2]paracyclophanes in good yields (Scheme 8). The cationic ruthenium(II) complex **27** is air- and moisture stable for weeks as solid and as solution in acetonitrile. Through coordination of ruthenium(II) to the ligand **8**, an additional stereogenic centre is generated, resulting in two possible diastereomers for **27**. As with the neutral complex **26**, only one diastereomer was observed for **27** via <sup>1</sup>H and <sup>13</sup>C NMR spectroscopy, indicating again the diastereoselective formation of the diastereomer with the *p*-cymene ligand pointing away from the [2.2]paracyclophane backbone.

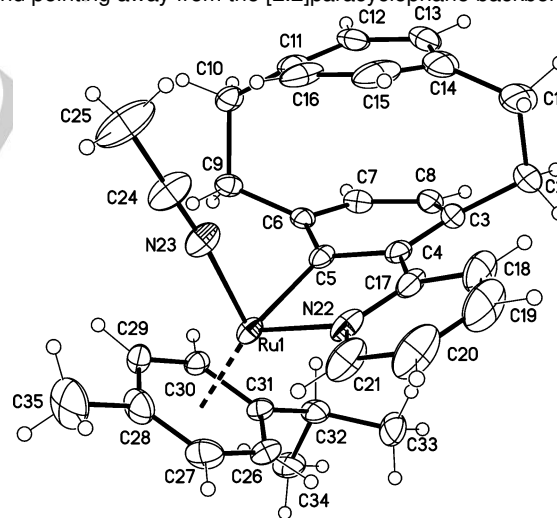
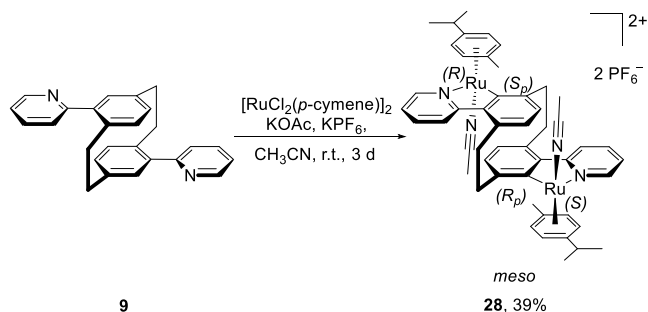


Figure 5: Molecular structure of **27** (displacement parameters are drawn at 50% probability level). For clarity the anion has been removed. Characteristic bond lengths: Ru–N<sup>Py</sup> 2.046(3) Å; Ru–C<sup>PC</sup> 2.057(4) Å; Ru–N<sup>MeCN</sup> 2.077(3) Å; Ru–C<sup>cymene</sup> 2.185(4)–2.302(4) Å, Ru–cymene 1.726(4) Å. Characteristic bond angles: N<sup>Py</sup>–Ru–C<sup>PC</sup> 76.95(14)°, N<sup>Py</sup>–Ru–N<sup>MeCN</sup> 85.61(13)°, N<sup>MeCN</sup>–Ru–C<sup>PC</sup> 91.04(14)°, N<sup>Py</sup>–Ru–cymene 132.1(2)°, N<sup>MeCN</sup>–Ru–cymene 127.2(2)°, C<sup>PC</sup>–Ru–cymene 127.8(2)°. PC = [2.2]paracyclophane.

From the cationic complex **27** we could obtain single crystals that were suitable for X-ray crystallography and confirm the stated molecular structure of (*R<sub>p</sub><sup>\*</sup>,S<sup>\*</sup>*)-**27** that is depicted in Figure 5. In

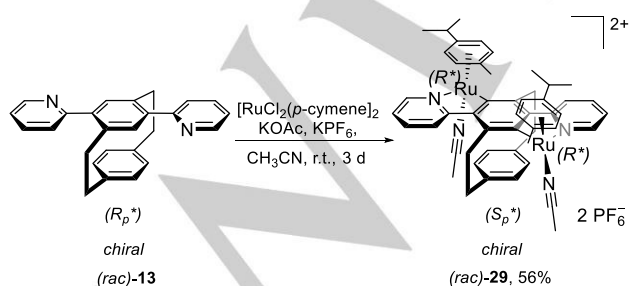
## FULL PAPER

the cationic complex **27**, the twist of the pyridyl ring against the [2.2]paracyclophane is significantly smaller compared to the free ligand with angles of 16.4° and 37.4°, respectively. The coordination geometry around the ruthenium(II) centre shows the expected piano stool and can be described as pseudo-tetrahedral. The  $N^{Py}-Ru-C^{PC}$  angle [76.95(14)°] is significantly smaller than the  $N^{Py}-Ru-N^{MeCN}$  and the  $C^{PC}-Ru-N^{MeCN}$  angle [85.61(13)° and 91.04(14)°]. These observations are most widely in agreement with those of cycloruthenated 2-phenylpyridine,<sup>[19c, 21e]</sup> but with a more distorted ruthenapyrrole in **27**. A characteristic of **27** is the shorter  $Ru-N^{Py}$  bond [2.046(3) Å] compared to those in the literature.



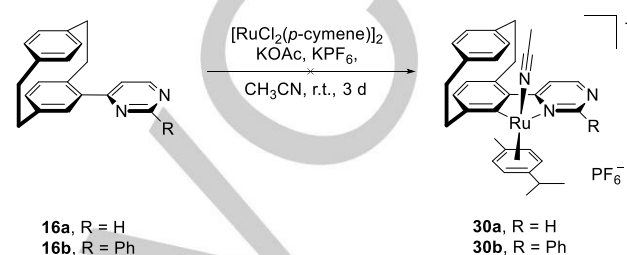
**Scheme 9:** Synthesis of the dinuclear ruthenium complex **28** from achiral **9**.

For the synthesis of homobimetallic complexes, we subjected the pseudo-*para*-bispyridyl-substituted [2.2]paracyclophane **9** to the analogous cycloruthenation conditions. After the reaction of the achiral **9** with  $[RuCl_2(p\text{-cymene})]_2$  the dinuclear ruthenium(II) complex **28** was isolated in 39% yield (**Scheme 9**). Due to the pseudo-tetrahedral coordinated ruthenium, two additional stereogenic centres are generated while the planar chirality of the [2.2]paracyclophane stays unaffected. In principle the formation of four configuration isomers is possible. However, the  $^{13}C$  NMR spectrum of **28** shows only 25 signals for the 50 carbon atoms in the molecule referring to a higher symmetry in the molecule and therefore chemically equivalent phenyl rings of the [2.2]paracyclophane as well as *p*-cymene and acetonitrile ligands. The assumption that the *p*-cymene ligands in **28** point away from the sterically demanding [2.2]paracyclophane backbone is in agreement with the observed molecular structure of **27** and an achiral *meso*-compound **28** with an inversion centre is obtained.



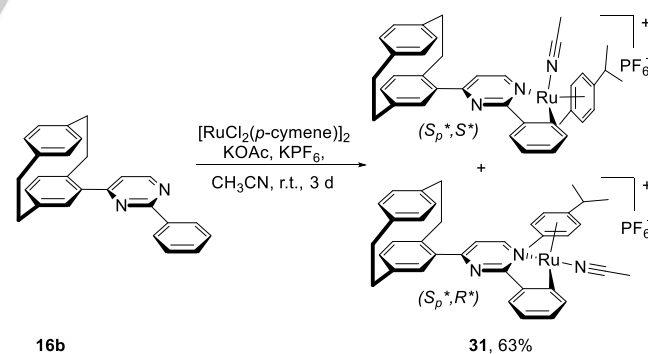
**Scheme 10:** Synthesis of the dinuclear ruthenium complex **29** from the chiral *para*-disubstituted (*rac*)-**13**. The relative configuration is shown.

Moreover, the chiral *para*-bispyridyl-substituted [2.2]paracyclophane **13** can also undergo cycloruthenation under comparable reaction conditions in 56% yield. The dinuclear ruthenium complex **29** could also form a mixture of diastereomers, analogous to those discussed above. This might be further compounded by the fact bispyridine **13** is chiral but a racemate. The NMR spectra suggest that a single,  $C_2$ -symmetric, diastereomer is formed (**Scheme 10**). As the racemic ligand (*rac*)-**13** was used, only the relative configuration is discussed.



**Scheme 11:** Attempted cycloruthenation of pyrimidyl-substituted [2.2]paracyclophanes **16** to yield complexes **30**.

Next, we subjected the pyrimidyl-substituted [2.2]paracyclophanes to the cycloruthenation conditions (**Scheme 11**). For the unsubstituted pyrimidine **16a**, no conversion of the ligand to a ruthenium complex could be observed. The phenyl-substituted pyrimidine **16b** does undergo C-H activation with  $[RuCl_2(p\text{-cymene})]_2$  but not at the desired position. Instead reaction occurs at the *ortho*-position of the phenyl ring. Based on  $^1H$  and  $^{13}C$  NMR spectroscopy it appears that reaction occurs with complete regioselectivity but gives a 1:1 mixture of the two possible diastereomers differing by the relative stereochemistry between the [2.2]paracyclophane and the metal centre (please see supporting information for detailed information).



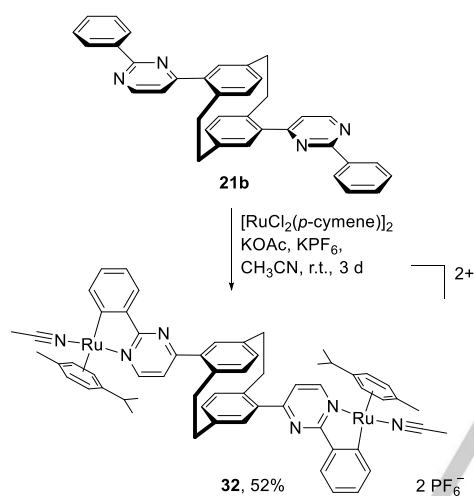
**Scheme 12:** Suggested structure of the obtained ruthenium(II) complex **31** after C-H activation of the phenyl substituent.

For the formation of two isomers, two possibilities have to take into account, with a regioselective but not diastereoselective reaction as the first option. The alternative is a not regioselective but diastereoselective reaction. Based on steric considerations with regards to bulky substituents and directing groups together

## FULL PAPER

with the observed 1:1 ratio and a lack of cross peaks between the protons of the [2.2]paracyclophane backbone and the *p*-cymene ligand in a NOESY NMR experiment, a regioselective reaction for the *N1'* nitrogen atom combined with a not diastereoselective reaction to a complex **31** seems to be the most probable option (Scheme 12, see supporting information for more details).

The observed behaviour of the pyrimidyl-substituted [2.2]paracyclophanes **16** in the cycloruthenation reaction shows the decreased reactivity for C-H activation of the [2.2]paracyclophane derivatives compared to the phenyl analogues. Another evidence is the low yield of the neutral complex **26** compared to the phenyl analogue **3**. The decreased reactivity might be explained by a combination of steric and electronic effects of the electron-rich, bulky [2.2]paracyclophane scaffold that impede addition of the ruthenium and the proposed intermolecular deprotonation<sup>[10b, 22]</sup>.



**Scheme 13:** Cycloruthenation of the pseudo-*para* bispyrimidyl-substituted [2.2]paracyclophane **21b**.

However, we wanted to synthesize the respective dinuclear complex of the bispyrimidyl-substituted [2.2]paracyclophane **21b** (Scheme 13). Therefore we used the analogous reaction conditions and observed again the C-H-activation of the phenyl substituents for the dinuclear product **32**. Similar to the pseudo-*para* bispyrimidyl-substituted [2.2]paracyclophane **9**, the ligand **21b** itself is achiral. Analogous to **28**, two new stereogenic centres are formed via pseudo-tetrahedral coordination of two ruthenium(II) centres while the planar-chiral configuration at the [2.2]paracyclophane is retained. That enables the formation of three diastereomers (see supporting information for details) that are distinguishable by NMR spectroscopy. Indeed, the NMR spectra of **32** displays only the double amount of signals referring to the number of atoms with a ratio of 1:1 and is exemplarily shown for some aromatic carbon atoms (Figure 6). If the statistical formation of the possible stereoisomers is assumed, all of them should be generated with the same probability. For the two chiral configuration isomers one signal is obtained per atom of the molecule. As enantiomers are not distinguishable via NMR spectroscopy, they result in a full signal set with double intensity. In contrast, the

two *meso* compounds both have an inversion centre which result in only half the amount of signals with double intensity. In summary the signals for the three diastereomers seem to be a "double signal set" with a 1:1 ratio which is visualized in Figure 6.

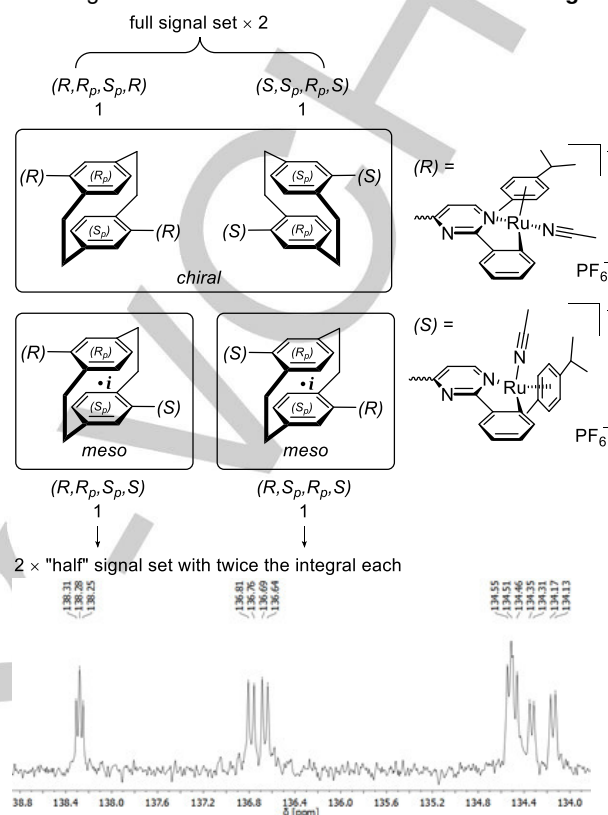
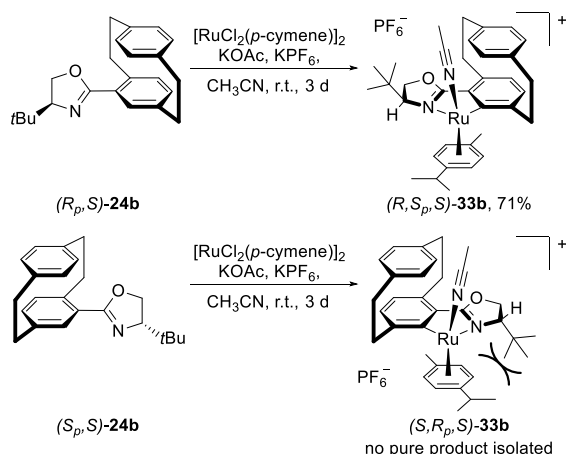


**Figure 6:** Verification of the observed number of signals in the NMR spectra of **32** (top) and an enlarged section of the aromatic region of the <sup>13</sup>C NMR spectrum of **32** (bottom).

Finally, we tested the oxazolonyl-substituted [2.2]paracyclophanes for their ability to coordinate ruthenium(II). As with 2-phenylpyridine, for 2-phenyloxazoline various cycloruthenated complexes are known.<sup>[11, 19c, 22-23]</sup> We subjected the *tert*-butyl-substituted oxazoline **24b** the cycloruthenation conditions, as only this oxazoline that was obtained diastereomerically pure. For the formation of the respective ruthenium complexes, a reactivity dependent on the used diastereomer was observed. Thus we isolated the ruthenium complex (*R,S<sub>p</sub>*)-**33b** by reaction of (*R<sub>p</sub>*,*S*)-**24b** in good yield of 71% whereas with the diastereomeric (*S<sub>p</sub>*,*S*)-**24b** we obtained only a mixture of several unidentifiable species (Scheme 14). This result can be explained by the spatial arrangement of the *tert*-butyl group relative to the [2.2]paracyclophane backbone and the *p*-cymene ligand. Reaction of (*R<sub>p</sub>*,*S*)-**24b** gives the diastereomeric complex (*R,S<sub>p</sub>*)-**33b** in which the *tert*-butyl substituent points towards the small acetonitrile ligand. This is readily accommodated. The (*S<sub>p</sub>*,*S*)-diastereomer would result in the formation of a complex that had a highly disfavoured non-bonding interaction between the *tert*-butyl group and the *p*-cymene ligand. As a result, this complex does not form and a series of side-reaction occurs instead.

## FULL PAPER



**Scheme 14:** Synthesis of the ruthenium complex **33b** from diastereomeric oxazolines **24b**.

From a sample of  $(R,S_p,S)$ -**33b** we were able to grow single crystals that were suitable for X-ray crystallography. Interestingly the obtained molecular structure from one of these crystals does not show the structure of  $(R,S_p,S)$ -**33b** that was determined by NMR spectroscopy and mass spectrometry, but a tri-cationic molecule  $(R,S_p,S)$ -**34** with two coordinated ruthenium(II) units.

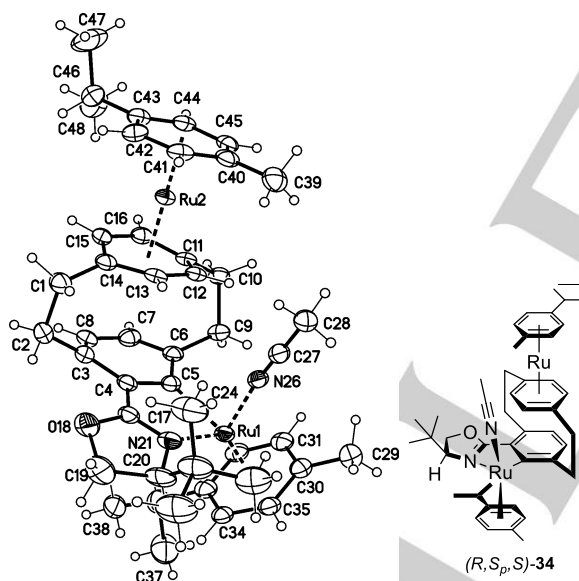
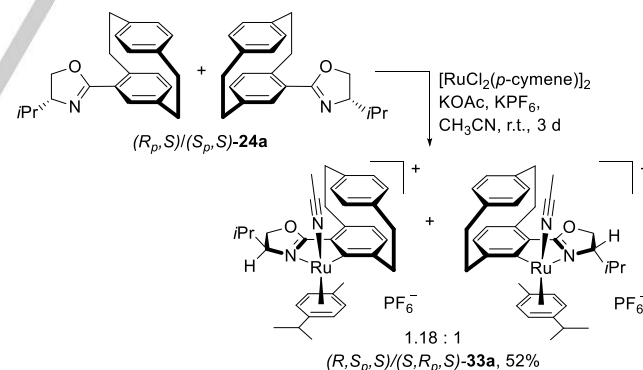


**Figure 7:** Instead the determined structure of **33b**, the measured crystal showed a tri-cationic dinuclear ruthenium complex **34** in X-ray crystallography (displacement parameters are drawn at 50% probability level). For clarity only one of the two independent molecules per unit cell is shown and the  $\text{PF}_6^-$  counter ions and solvent have been removed. Characteristic bond lengths for both independent molecules:  $\text{Ru}-\text{N}^{\text{Ox}}$  2.120(8) and 2.093(8) Å;  $\text{Ru}-\text{C}^{\text{PC}}$  2.083(9) and 2.085(10) Å;  $\text{Ru}-\text{N}^{\text{MeCN}}$  2.059(8) and 2.067(9) Å;  $\text{Ru}-\text{C}^{\text{cymene}}$  2.164(10)–2.279(10) and 2.167(9)–2.293(11) Å,  $\text{Ru}^2-\text{C}^{\text{PC}}$  2.203(9)–2.353(8) and 2.199(11)–2.375(10) Å;  $\text{Ru}^2-\text{C}^{\text{cymene}^2}$  2.190(9)–2.243(9) and 2.202(11)–2.254(12) Å. Characteristic bond angles:  $\text{N}^{\text{Ox}}-\text{Ru}-\text{C}^{\text{PC}}$  78.2(3)° and 78.2(3)°,  $\text{N}^{\text{Ox}}-\text{Ru}-\text{N}^{\text{MeCN}}$  85.2(3)° and 85.8(3)°,  $\text{N}^{\text{MeCN}}-\text{Ru}-\text{C}^{\text{PC}}$  90.3(3)° and 91.1(3)°. The oxazolanyl unit and the [2.2]paracyclophane are twisted by 14.7° and 19.9° against each other.

The dinuclear complex  $(R,S_p,S)$ -**34** possesses a cycloruthenated oxazolanyl-substituted [2.2]paracyclophane but with a second ruthenium(II) center that is  $\eta^6$ -coordinated by the second deck of the [2.2]paracyclophane forming a sandwich-type complex (**Figure 7**). [2.2]Paracyclophanes as  $\eta^6$ -coordinating arene ligands for ruthenium(II) are known since the initial reports particularly by Boekelheide *et al.*<sup>[24]</sup> in the 1980s and have been extensively studied.<sup>[25]</sup> Nevertheless, among the numerous examples of a cycloruthenation with  $\text{KPF}_6$  to a cationic complex, the literature presents only a single report for the formation of a similar tri-cationic product.<sup>[26]</sup> This complex was formed as further reaction of a cyclometallated 2-phenylpyridine derivative with another  $(\eta^6\text{-benzene})\text{Ru}^{2+}$  fragment that is only occurring for cycloruthenation products with sufficient instability. The equilibrium can be shifted towards the tri-cation by an excess of the ruthenium(II) precursor.<sup>[26]</sup> But unfortunately, all our attempts to a targeted synthesis of **34** by an excess of  $[\text{RuCl}_2(p\text{-cymene})]_2$  were unsuccessful and gave only the cycloruthenated di-cationic mononuclear complex, which was also the case for the reaction of the pyridyl-substituted **8** with an excess  $[\text{RuCl}_2(p\text{-cymene})]_2$ . That prompts the conclusion that the tri-cationic dinuclear complex is a decomposition product that was formed during the crystallization process, which was not performed under argon atmosphere.

Hoping that only one diastereomer reacts, we subjected the inseparable diastereomeric mixture of **24a** for the cycloruthenation. Ideally only the  $(R_p,S)$ -**24a** diastereomer would react analogous to the observed reactivity for the diastereomers of **24b** in a diastereoselective reaction, so that only one of the diastereomeric products **33a** would be formed (**Scheme 15**). Indeed, only the product of the non-diastereoselective cycloruthenation could be obtained with a ratio of 1.18:1. This is explainable by the smaller and more flexible isopropyl group compared to the bulky *tert*-butyl group that is able to avoid steric hindrance by rotation.

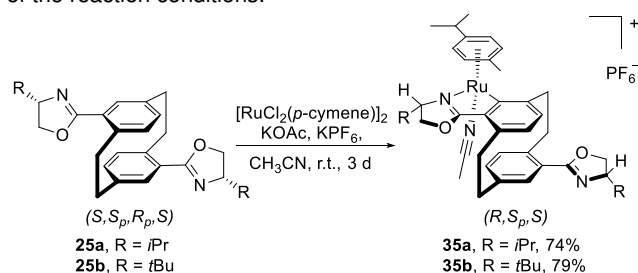


**Scheme 15:** Synthesis of the ruthenium(II) complex **33a** starting from oxazoline **24a** as diastereomeric mixture.

Afterwards we investigated the reaction of  $[\text{RuCl}_2(p\text{-cymene})]_2$  with the pseudo-*para*-bisoxazolines **25**. These molecules features both, a  $(R_p)$ - and a  $(S_p)$ -configured ring combined with an  $(S)$ -oxazoline ring that possesses an isopropyl or a *tert*-butyl substituent. In both cases, only the mononuclear ruthenium complexes **35** was isolated in good yields (>74%, **Scheme 16**), which is consistent with the above-mentioned reactivity for the two

## FULL PAPER

diastereomeric *tert*-butylsubstituted monooxazolines **24b**. For the bisoxazolines **25**, only the (*R<sub>p</sub>*)-ring of the [2.2]paracyclophane in combination with the (*S*)-configuration of the oxazoline as starting material enables the stable coordination to the ruthenium metal. However, this result seems surprising regarding the observed reactivity for the [2.2]paracyclophane-based bisoxazoline **25a** with *isopropyl* substituents, as the respective diastereomeric monooxazolines **24a** do not show diastereospecific cycloruthenation upon reaction with [RuCl<sub>2</sub>(*p*-cymene)]<sub>2</sub>. Therefore, ongoing research in our laboratories is necessary to figure out if a diastereoselective reaction for the monooxazoline **24a** or the double cycloruthenation of **25a** is obtained by further optimization of the reaction conditions.



**Scheme 16:** Reaction of the pseudo-*para* bisoxazolines **25** to the mononuclear ruthenium complexes **35**.

## Conclusions

The planar-chiral [2.2]paracyclophane backbone is a versatile hydrocarbon scaffold that enables the synthesis of unique 3D architectures due to its unique molecular geometry. Therefore we explored synthetic routes to pseudo-*para*- or *para*-disubstituted [2.2]paracyclophanes with additional *N*-donor groups such as pyridines, pyrimidines and oxazolines. By subjecting the obtained *N*-donor-substituted [2.2]paracyclophanes to common cycloruthenation conditions under C-H activation, it can be stated that the potential of the [2.2]paracyclophane to undergo cycloruthenation is obviously inferior to a phenyl ring. Thus, only the cationic ruthenium complexes of substituted [2.2]paracyclophanes could be isolated in satisfactory yields. In case of a 2-pyridyl substituent as *N*-donor, the cycloruthenation proceeded diastereoselectively at the pseudo-tetrahedral coordinated ruthenium centre, preferring the configuration where the *p*-cymene ligand points away from the [2.2]paracyclophane backbone. For a pyrimidine substituent as *N*-donor, no cycloruthenation of the [2.2]paracyclophane backbone took place, but instead the C-H activation of a simple aromatic substituent at the pyrimidine. For oxazoline substituents diastereoselective cycloruthenation was observed that was in addition diastereoselective for oxazolines with a bulky *tert*-butyl substituent.

In summary we showed that substituted [2.2]paracyclophanes are able to act as bridging ligands for dinuclear ruthenium complexes if substituted with a suitable *N*-donor ligand. This enables the synthesis of rigid dinuclear complexes with defined distance and orientation between the two metal centres which are not accessible by commonly used planar ligand structures.

## Experimental Section

**General cycloruthenation reaction to the cationic complexes:** In a schlenk tube the [2.2]paracyclophane-based ligand (1.00 equiv.), [RuCl<sub>2</sub>(*p*-cymene)]<sub>2</sub> (1.00 equiv. or 0.50 equiv.), KOAc (1.50 equiv. or 3.00 equiv.) and KPF<sub>6</sub> (2.00 equiv. 1.50 equiv.) in dry acetonitrile (5 mL) were stirred at r.t. for 3 d. The solvent was removed under reduced pressure and the residue was purified by column chromatography on silica gel (cyclohexane/ethyl acetate 50/50 → acetonitrile) to obtain the ruthenium complex as yellow solid.

## Crystal Structure Determinations

The single-crystal X-ray diffraction study was carried out on an Agilent SuperNova diffractometer with EOS detector at 173(2) K using Mo-K $\alpha$  radiation ( $\lambda = 0.71073 \text{ \AA}$ , **12**), a Bruker D8 Venture diffractometer with Photon100 detector at 123(2) K using Cu-K $\alpha$  radiation ( $\lambda = 1.54178 \text{ \AA}$ , **13**, **16a**, **34**) or using Mo-K $\alpha$  radiation ( $\lambda = 0.71073 \text{ \AA}$ , **21b**, **27**) and a Bruker-Nonius KappaCCD at 123(2) K using Mo-K $\alpha$  radiation ( $\lambda = 0.71073 \text{ \AA}$ , **18**, **19**). Direct Methods (SHELXS-97)<sup>[27]</sup> or dual space methods (SHELXT for **27**, **34**)<sup>[28]</sup> were used for structure solution and refinement was carried out using SHELXL-2013 or SHELXL-2014 (full-matrix least-squares on  $F^2$ )<sup>[29]</sup>. Hydrogen atoms were localized by difference electron density determination and refined using a riding model. An analytical absorption correction was applied for **12**, semi-empirical absorption corrections were applied for **13**, **16a**, **18**, **19**, **21b**, **27** and **34**. For **13** and **16a** an extinction correction was applied. The absolute structure of **27** and the absolute configuration of **34** were determined by refinement of Parsons' *x*-parameter<sup>[30]</sup>. In **19** are 2 x 0.5 molecules and one complete molecule in the asymmetric unit, in the complete molecule one acetyl O-atom is disordered. In **27** and **34**, respectively one anion PF<sub>6</sub><sup>-</sup> is disordered. In **27** the anion (due to the symmetry of the space group) is localized on three positions, one ordered, one disordered and on the third position the refinement with the listed atoms show residual electron density due to a heavily disordered PF<sub>6</sub><sup>-</sup> anion which could not be refined with split atoms. Therefore the option "SQUEEZE" of the program package PLATON<sup>[31]</sup> was used to create a hkl file taking into account the residual electron density in the void areas. Therefore the atoms list and unit card do not agree. In **34** the refinement with the listed atoms show residual electron density due to three heavily disordered water molecules which could not be refined with split atoms. The option "SQUEEZE" of the program package PLATON<sup>[31]</sup> was used to create an hkl file taking into account the residual electron density in the void areas. The water molecules are not included in the atoms list and unit card (for the refinement of the disorder and SQUEEZE of **27** and **34** see the cif-file for details).

**13:** colourless crystals, C<sub>26</sub>H<sub>22</sub>N<sub>2</sub>, *M<sub>r</sub>* = 362.45, crystal size 0.24 × 0.20 × 0.08 mm, orthorhombic, space group *Pccn* (No. 56), *a* = 11.6872(4) Å, *b* = 42.5118(13) Å, *c* = 7.3758(2) Å, *V* = 3664.6(2) Å<sup>3</sup>, *Z* = 8,  $\rho$  = 1.314 Mg/m<sup>3</sup>,  $\mu$ (Cu-K $\alpha$ ) = 0.589 mm<sup>-1</sup>, *F*(000) = 1536,  $2\theta_{\max}$  = 144.4°, 22288 reflections, of which 3600 were independent (*R<sub>int</sub>* = 0.025), 254 parameters, *R<sub>1</sub>* = 0.037 (for 3362 *I* > 2 $\sigma$ (*I*)), *wR<sub>2</sub>* = 0.098 (all data), *S* = 1.03, largest diff. peak / hole = 0.275 / -0.170 e Å<sup>-3</sup>.

**21b:** colourless crystals, C<sub>36</sub>H<sub>28</sub>N<sub>4</sub> · CH<sub>2</sub>Cl<sub>2</sub>, *M<sub>r</sub>* = 601.55, crystal size 0.16 × 0.14 × 0.02 mm, triclinic, space group *P-1* (No. 2), *a* = 7.2898(4) Å, *b* = 13.8443(8) Å, *c* = 15.2534(9) Å,  $\alpha$  = 73.925(3)°,  $\beta$  = 77.739(2)°,  $\gamma$  = 78.526(2)°, *V* = 1429.29(14) Å<sup>3</sup>, *Z* = 2,  $\rho$  = 1.398 Mg/m<sup>3</sup>,  $\mu$ (Mo-K $\alpha$ ) = 0.263 mm<sup>-1</sup>, *F*(000) = 628,  $2\theta_{\max}$  = 55.2°, 50346 reflections, of which 6589 were independent (*R<sub>int</sub>* = 0.049), 388 parameters, *R<sub>1</sub>* = 0.038 (for 5433 *I* > 2 $\sigma$ (*I*)), *wR<sub>2</sub>* = 0.098 (all data), *S* = 1.02, largest diff. peak / hole = 0.310 / -0.453 e Å<sup>-3</sup>.

## FULL PAPER

**27:** yellow crystals,  $C_{33}H_{35}N_2Ru \cdot PF_6$ ,  $M_r = 705.67$ , crystal size  $0.22 \times 0.18 \times 0.12$  mm, trigonal, space group  $P31c$  (No. 159),  $a = 17.0065(6)$  Å,  $c = 18.2539(6)$  Å,  $V = 4572.1(4)$  Å<sup>3</sup>,  $Z = 6$ ,  $\rho = 1.538$  Mg/m<sup>3</sup>,  $\mu(Mo-K\alpha) = 0.630$  mm<sup>-1</sup>,  $F(000) = 2160$ ,  $2\theta_{max} = 55.2^\circ$ , 91047 reflections, of which 6947 were independent ( $R_{int} = 0.033$ ), 371 parameters, 1 restraint,  $R_1 = 0.028$  (for 6709  $I > 2\sigma(I)$ ),  $wR_2 = 0.068$  (all data),  $S = 1.07$ , largest diff. peak / hole =  $0.847 / -0.819$  e Å<sup>-3</sup>,  $x = -0.028(5)$ .

**34:** yellow crystals,  $C_{45}H_{57}N_2ORu_2 \cdot 3 PF_6 \cdot CHCl_3$ ,  $M_r = 1398.34$ , crystal size  $0.18 \times 0.10 \times 0.02$  mm, triclinic, space group  $P1$  (No. 1),  $a = 10.6537(3)$  Å,  $b = 15.7694(4)$  Å,  $c = 16.4628(4)$  Å,  $\alpha = 87.271(1)^\circ$ ,  $\beta = 85.346(1)^\circ$ ,  $\gamma = 81.364(1)^\circ$ ,  $V = 2723.66(12)$  Å<sup>3</sup>,  $Z = 2$ ,  $\rho = 1.705$  Mg/m<sup>3</sup>,  $\mu(Cu-K\alpha) = 7.574$  mm<sup>-1</sup>,  $F(000) = 1404$ ,  $2\theta_{max} = 144.8^\circ$ , 31716 reflections, of which 16299 were independent ( $R_{int} = 0.039$ ), 1344 parameters, 3409 restraints,  $R_1 = 0.055$  (for 15521  $I > 2\sigma(I)$ ),  $wR_2 = 0.147$  (all data),  $S = 1.03$ , largest diff. peak / hole =  $2.333$  (near Ru atoms) /  $-1.030$  (near disordered P-atom) e Å<sup>-3</sup>,  $x = -0.034(9)$ .

CCDC 1558680 (**12**), 1558681 (**13**), 1558682 (**16a**), 1558683 (**18**), 1558684 (**19**), 1558685 (**21b**), 1558686 (**27**), and 1558687 (**34**) contain the supplementary crystallographic data for this paper. These data can be obtained free of charge from The Cambridge Crystallographic Data Centre via [www.ccdc.cam.ac.uk/data\\_request/cif](http://www.ccdc.cam.ac.uk/data_request/cif).

## Acknowledgements

We thank the SFB/TR 88 for financial support and N. B. Heine for his help with the synthesis of **12**. C. B. gratefully acknowledges the Evonik Stiftung for financial support.

**Keywords:** Cyclophanes • Ruthenium • Chirality • Diastereoselectivity • Metallacycle

- [1] C. J. Brown, A. C. Farthing, *Nature* **1949**, *164*, 915-916.
- [2] a) H. J. Reich, D. J. Cram, *J. Am. Chem. Soc.* **1967**, *89*, 3078-3080; b) H. J. Reich, D. J. Cram, *J. Am. Chem. Soc.* **1968**, *90*, 1365-1367; c) H. J. Reich, D. J. Cram, *J. Am. Chem. Soc.* **1969**, *91*, 3534-3543; d) H. J. Reich, D. J. Cram, *J. Am. Chem. Soc.* **1969**, *91*, 3527-3533; e) H. J. Reich, D. J. Cram, *J. Am. Chem. Soc.* **1969**, *91*, 3517-3526; f) H. J. Reich, D. J. Cram, *J. Am. Chem. Soc.* **1969**, *91*, 3505-3516.
- [3] O. R. P. David, *Tetrahedron* **2012**, *68*, 8977-8993.
- [4] D. J. Cram, J. M. Cram, *Acc. Chem. Res.* **1971**, *4*, 204-213.
- [5] a) S. E. Gibson, J. D. Knight, *Org. Biomol. Chem.* **2003**, *1*, 1256-1269; b) S. Bräse, S. Dahmen, S. Höfener, F. Lauterwasser, M. Kreis, R. E. Ziegert, *Synlett* **2004**, 2647-2669; c) G. J. Rowlands, *Org. Biomol. Chem.* **2008**, *6*, 1527-1534; d) J. Paradies, *Synthesis* **2011**, 3749-3766; e) G. J. Rowlands, *Isr. J. Chem.* **2012**, *52*, 60-75.
- [6] a) H. Hopf, *Angew. Chem. Int. Ed.* **2008**, *47*, 9808-9812; *Angew. Chem.* **2008**, *120*, 9954-9958; b) E. Elacqua, L. R. MacGillivray, *Eur. J. Org. Chem.* **2010**, 6883-6894.
- [7] C. Bolm, K. Wenz, G. Raabe, *J. Organomet. Chem.* **2002**, *662*, 23-33.
- [8] a) J. R. Fulton, J. E. Glover, L. Kamara, G. J. Rowlands, *Chem. Commun.* **2011**, 47, 433-435; b) C. Braun, E. Spuling, N. B. Heine, M. Kacici, M. Nieger, S. Bräse, *Adv. Synth. Catal.* **2016**, *358*, 1664-1670.
- [9] J. E. Glover, P. G. Plieger, G. J. Rowlands, *Aust. J. Chem.* **2014**, *67*, 374-380.
- [10] a) J.-P. Djukic, A. Berger, M. Duquenne, M. Pfeffer, A. de Cian, N. Kyritsakas-Gruber, J. Vachon, J. Lacour, *Organometallics* **2004**, *23*, 5757-5767; b) E. Ferrer Flegeau, C. Bruneau, P. H. Dixneuf, A. Jutand, *J. Am. Chem. Soc.* **2011**, *133*, 10161-10170.
- [11] D. L. Davies, O. Al-Duaij, J. Fawcett, K. Singh, *Organometallics* **2010**, *29*, 1413-1420.
- [12] a) G. J. Rowlands, R. J. Seacome, *Beilstein J. Org. Chem.* **2009**, *5*, No. 9; b) A. Pelter, H. Kidwell, R. A. N. C. Crump, *J. Chem. Soc., Perkin Trans.* **1997**, 1317-13140; c) M. Brink, *Synthesis* **1975**, 807-808.
- [13] a) E. Bejan, H. A. Haddou, J. C. Daran, G. G. A. Balavoine, *Synthesis* **1996**, 1012-1018; b) F. Pezet, L. Routaboul, J.-C. Daran, I. Sasaki, H. Ait-Haddou, G. G. A. Balavoine, *Tetrahedron* **2000**, *56*, 8489-8493; c) K. Muller, A. Schubert, T. Jozak, A. Ahrens-Botzong, V. Schünemann, W. R. Thiel, *ChemCatChem* **2011**, *3*, 887-892; d) L. Taghizadeh Ghoochany, C. Kerner, S. Farsadpour, F. Menges, Y. Sun, G. Niedner-Schatteburg, W. R. Thiel, *Eur. J. Inorg. Chem.* **2013**, 4305-4317.
- [14] M. Busch, M. Cayir, M. Nieger, W. R. Thiel, S. Bräse, *Eur. J. Org. Chem.* **2013**, 6108-6123.
- [15] a) E. A. Truesdale, D. J. Cram, *J. Org. Chem.* **1980**, *45*, 3974-3981; b) J. E. Gready, T. W. Hambley, K. Kakiuchi, K. Kobiro, S. Sternhell, C. W. Tansey, Y. Tobe, *J. Am. Chem. Soc.* **1990**, *112*, 7537-7540.
- [16] V. I. Rozenberg, N. V. Dubrovina, E. V. Vorontsov, E. V. Sergeeva, Y. N. Belokon', *Tetrahedron: Asymmetry* **1999**, *10*, 511-517.
- [17] A. Marchand, A. Maxwell, B. Mootoo, A. Pelter, A. Reid, *Tetrahedron* **2000**, *56*, 7331-7338.
- [18] H. Allgeier, M. G. Siegel, R. C. Helgeson, E. Schmidt, D. J. Cram, *J. Am. Chem. Soc.* **1975**, *97*, 3782-3789.
- [19] a) Q. Yu, L. Hu, Y. Wang, S. Zheng, J. Huang, *Angew. Chem. Int. Ed.* **2015**, *54*, 15284-15288; *Angew. Chem.* **2015**, *127*, 15499-15503; b) A. J. Paterson, S. St John-Campbell, M. F. Mahon, N. J. Press, C. G. Frost, *Chem. Commun.* **2015**, *51*, 12807-12810; c) B. Li, C. Darcel, T. Roisnel, P. H. Dixneuf, *J. Organomet. Chem.* **2015**, *793*, 200-209; d) N. Hofmann, L. Ackermann, *J. Am. Chem. Soc.* **2013**, *135*, 5877-5884.
- [20] a) H. C. L. Abbenhuis, M. Pfeffer, J. P. Sutter, A. de Cian, J. Fischer, H. L. Ji, J. H. Nelson, *Organometallics* **1993**, *12*, 4464-4472; b) S. Attar, J. H. Nelson, J. Fischer, A. de Cian, J.-P. Sutter, M. Pfeffer, *Organometallics* **1995**, *14*, 4559-4569; c) M. Pfeffer, J.-P. Sutter, E. P. Urriolabeitia, *Inorg. Chim. Acta* **1996**, *249*, 63-67.
- [21] a) S. Fernandez, M. Pfeffer, V. Ritteng, C. Sirlin, *Organometallics* **1999**, *18*, 2390-2394; b) B. Boff, M. Ali, L. Alexandrova, N. A. Espinosa-Jalapa, R. O. Saavedra-Diaz, R. Le Lagadec, M. Pfeffer, *Organometallics* **2013**, *32*, 5092-5097; c) A. D. Ryabov, V. S. Sukharev, L. Alexandrova, R. Le Lagadec, M. Pfeffer, *Inorg. Chem.* **2001**, *40*, 6529-6532; d) R. Le Lagadec, L. Rubio, L. Alexandrova, R. A. Toscano, E. V. Ivanova, R. Meškys, V. Laurinavičius, M. Pfeffer, A. D. Ryabov, *J. Organomet. Chem.* **2004**, *689*, 4820-4832; e) V. Martínez Cornejo, J. Olvera Mancilla, S. López Morales, J. A. Oviedo Fortino, S. Hernández-Ortega, L. Alexandrova, R. Le Lagadec, *J. Organomet. Chem.* **2015**, *799-800*, 299-310.
- [22] I. Fabre, N. von Wolff, G. Le Duc, E. Ferrer Flegeau, C. Bruneau, P. H. Dixneuf, A. Jutand, *Chem. Eur. J.* **2013**, *19*, 7595-7604.
- [23] a) Y. Boutadla, D. L. Davies, R. C. Jones, K. Singh, *Chem. Eur. J.* **2011**, *17*, 3438-3448; b) W.-G. Jia, T. Zhang, D. Xie, Q.-T. Xu, S. Ling, Q. Zhang, *Dalton Trans.* **2016**, *45*, 14230-14237.
- [24] a) E. D. Laganis, R. G. Finke, V. Boekelheide, *Tetrahedron Lett.* **1980**, *21*, 4405-4408; b) R. T. Swann, V. Boekelheide, *Tetrahedron Lett.* **1984**, *25*, 899-900; c) R. T. Swann, A. W. Hanson, V. Boekelheide, *J. Am. Chem. Soc.* **1984**, *106*, 818-819; d) R. T. Swann, A. W. Hanson, V. Boekelheide, *J. Am. Chem. Soc.* **1986**, *108*, 3324-3334.
- [25] a) M. R. J. Elsegood, D. A. Tocher, *J. Organomet. Chem.* **1988**, *356*, C29-C31; b) M. R. J. Elsegood, D. A. Tocher, *Inorg. Chim. Acta* **1989**, *161*, 147-149; c) M. R. J. Elsegood, J. W. Steed, D. A. Tocher, *J. Chem. Soc., Dalton Trans.* **1992**, 1797-1801; d) P. J. Dyson, B. F. G. Johnson, C. M. Martin, A. J. Blake, D. Braga, F. Grepioni, E. Parisini, *Organometallics* **1994**, *13*, 2113-2117; e) B. Gollas, B. Speiser, J. Sieglens, J. Strähle, *Organometallics* **1996**, *15*, 260-271; f) B. Gollas, B. Speiser, I. Zagoc, C. Maichle-Mössmer, *J. Organomet. Chem.* **2000**, *602*, 75-90; g) R. Bhalla, C. J. Boxwell, S. B. Duckett, P. J. Dyson, D. G. Humphrey, J. W. Steed, P. Suman, *Organometallics* **2002**, *21*, 924-928.
- [26] J.-P. Djukic, L. Fetzler, A. Czysz, W. Iali, C. Sirlin, M. Pfeffer, *Organometallics* **2010**, *29*, 1675-1679.
- [27] G. M. Sheldrick, *Acta Crystallogr. A* **2008**, *64*, 112-122.
- [28] G. M. Sheldrick, *Acta Crystallogr. A* **2015**, *71*, 3-8.
- [29] G. M. Sheldrick, *Acta Crystallogr. C* **2015**, *71*, 3-8.
- [30] S. Parsons, H. D. Flack, T. Wagner, *Acta Crystallogr. B* **2013**, *69*, 249-259.
- [31] A. Spek, *Acta Crystallogr. D* **2009**, *65*, 148-155.